ARMY RESEARCH LABORATORY

Models for Saturable and Reverse Saturable Absorption in Materials for Optical Limiting

by Timothy Pritchett

ARL-TR-2567 October 2002

The findings in this report are not to be construed as an official Department of the Army position unless so designated by other authorized documents.

Citation of manufacturer's or trade names does not constitute an official endorsement or approval of the use thereof.

Destroy this report when it is no longer needed. Do not return it to the originator.

Army Research Laboratory
Adelphi, MD 20783-1197

ARL-TR-2567 **October 2002**

Models for Saturable and Reverse Saturable Absorption in Materials for Optical Limiting

Timothy Pritchett

Sensors and Electron Devices Directorate, ARL

Models for Saturable and Reverse Saturable Absorption in Materials for Optical Limiting

Timothy Pritchett

Sensors and Electron Devices Directorate, ARL

Abstract

The systems used to protect eyes and sensors from frequency-agile laser weapons must be capable, over a relatively broad range of frequencies, of absorbing, refracting, deflecting, or scattering laser radiation of high intensity, even while affording high transmission to light of low to moderate intensity. The design of such devices begins with an accurate characterization of the nonlinear optical response of the candidate active materials. In this work, the relevant material parameters can be extracted from experimentally obtained data only by indirect means: that is, the actual experimental results are compared to the results obtained from a theoretical model employing hypothetical values of the desired parameters, and the parameters of the model are varied until the model results match the experimental data. If this procedure is to work, the model must capture all the essential features of the interaction of the material to be characterized with the laser beam propagating through it. We review the assumptions and approximations underlying the commonly used models for nonlinear absorption, paying particular to the limits of applicability that these impose.

Contents

Figures

Tables

1 Introduction

Over the years, the nonlinear optical response of an enormous variety of materials has been studied, the absorptive and refractive contributions to that response have been accurately measured and characterized, and the underlying physical mechanisms have been elucidated. Most materials exhibit *saturable absorption*: that is, they absorb the greatest fraction of the incident radiant power when the input fluence (total delivered energy per unit area) is low, with the absorption diminishing as the fluence increases. Physically, this occurs because the absorption cross-section for the ground state is greater than the absorption cross-section(s) for the excited state(s). The observed decrease in absorption with increasing fluence results simply from the depletion over time of the ground state population as an ever-increasing fraction of the absorber molecules is excited.

The opposite situation, in which the absorption cross section(s) of the excited state(s) exceeds that of the ground state, gives rise to *reverse saturable absorption* (RSA), in which the absorption *increases* with input fluence. This enhancement of absorption reflects the increase in the population of the (more strongly absorbing) excited state(s) relative to that of the (less strongly absorbing) ground state. First reported in the dyes sudanschwartz-B and indanthrone by Guiliano and Hess [1], RSA has since been observed in a variety of organic and organo-metallic molecules and complexes, including ion tricobalt clusters [2], King's complex [3], metallophthalocyanines [4], metallo-napthalocyanines [4, 5], fullerenes (C_{60}) [6-9], metallotetrabenzporphyrines [10], and cubane-like transition-metal clusters [11].

Both types of absorptive nonlinearity, saturable absorption as well as RSA, offer practical applications. For instance, saturable absorbers are commonly used as passive Q-switches in pulsed lasers. Materials exhibiting RSA, on the other hand, could be exploited in optical limiting applications such as eye and sensor protection systems, which require high transmission of low-intensity radiation but high absorption at high input [12, 13].

The same population redistribution responsible for absorptive nonlinearities also gives rise to changes in the refractive index. (One might expect this, since the leading-order nonlinear refractive index and nonlinear absorption coefficient are, respectively, the real and imaginary parts of the third-order nonlinear susceptibility and thus are linked by Kramers-Kronig relations [14].) A full characterization of the nonlinear optical response of a material involves the measurement of both absorptive and refractive nonlinearities. These two quantities are typically measured with *Z*-scan techniques [15, 16]. In a *Z*-scan experiment, a sample of material is moved from one side of focus to the other along the propagation path (*Z*) of a tightly focused Gaussian beam and the apertured and unapertured transmittance of the sample is measured as a function of the sample's position relative to focus. From the apertured transmittance curve ("closed aperture *Z*-scan"), one may deduce the sign and magnitude of the nonlinear refractive index; one then uses the unapertured transmittance data ("open aperture *Z*-scan") to infer the strength of the nonlinear absorption.

In characterizing optically nonlinear materials, one generally extract the relevant material parameters from experimentally obtained data only by indirect means: that is, the actual experimental results are compared to the results obtained from a theoretical model employing

hypothetical values of the desired parameters, and the parameters of the model are varied until the model results match the experimental data. If this procedure is to work, the model must capture all the essential features of the interaction of the material to be characterized with the laser beam propagating through it.

In this report, we review the existing models for nonlinear absorption, paying particular attention to the assumptions and approximations involved in each model and to the limits of applicability that these impose. We begin our review with a discussion of the analytic model presented by Wei et al. in one of the earliest papers on the open aperture *Z*-scan technique [4]. Inconsistencies in the assumptions that underlie the Wei model entrain numerous difficulties, but these problems are partially offset by the convenience of a fully analytic solution. Section 3 treats the next most complicated excited state absorption model. This model, though still very simple, can no longer be fully solved by purely analytic means in the general case. However, a complete analytic solution *is* possible in the limit of low fluence, and we outline this solution in Section 4. This is, to the best of our knowledge, a new result that does not appear in the literature, and it represents a definite improvement over the original model of Wei et al. In Section 5, we conclude our review of the simplest excited state absorption models with a comparative discussion of the three models described so far. In Section 6, we turn our attention to the so-called five-band model, a numerical model broadly applicable to porphyrins and other conjugated aromatic compounds. Section 7 introduces a commonly seen approximation in the five-band model, and Sections 8 and 9 assess the impact of this approximation. Section 10 describes further simplifications of the five-band model that are applicable in particular limits.

2 An Analytic Absorption Model: Excited State Absorption With Constant Ground State Absorption

Among the earliest theoretical treatments of excited state absorption is the following simplified model, in which the excited state is populated by linear absorption from the ground state [4]. In this model, the number density $n_1(t)$ of molecules in the excited state is given by

$$\frac{\partial n_1}{\partial t} = \frac{\alpha}{h\nu} I , \tag{1}$$

where ν is the frequency of the laser radiation, h is the Planck constant, and I the irradiance; α, the linear absorption coefficient, is a constant. The irradiance is determined by

$$\frac{\partial I}{\partial z} = -(\alpha + \sigma_1 n_1) I , \tag{2}$$

where σ_1 is the excited state absorption cross-section. Though highly problematic from a physical standpoint, the assumption of a purely linear ground state absorption process, completely characterized by the constant coefficient α, does possess one overwhelming virtue: the resulting model, given by Equations (1) and (2), can be solved analytically. One proceeds as follows. Introducing the total fluence,

$$F(r,z) = \int_{-\infty}^{\infty} I(r,z,t')\, dt' , \tag{3}$$

one integrates (1) and (2) over all time and combines the results to obtain

$$\frac{\partial F}{\partial z} = -\alpha F - \frac{\alpha \sigma_1}{2h\nu} F^2 . \tag{4}$$

For a sufficiently thin sample (one whose thickness L is much less than the Rayleigh range of the beam), one may disregard the diffraction of the beam as it propagates through the sample and so perform the longitudinal (z) integration of (4) over thickness of the sample. This yields a relation between the total fluence entering the sample at a radial distance r from the center of the beam and the exit fluence at the same r. In the case in which the input fluence results from a principal-mode Gaussian beam, this relation may be integrated over the transverse beam profile to give the total transmitted energy or, equivalently, the normalized transmittance T / T_{Linear}:

$$\frac{T}{T_{Linear}} = \frac{\ln[1+q]}{q} \tag{5}$$

Here, the dimensionless parameter q is given by

$$q = \frac{\alpha \sigma_1}{2h\nu} F_0 L_{eff} ,$$

where F_0 is the total fluence on-axis, and $L_{eff} = (1 - \exp[-\alpha L]) / \alpha$ is the effective sample thickness.

As we have already pointed out, the most glaring inconsistency in this simplified model is introduced by assumption that the rate of growth, αI, of the population density of molecules in the excited state depends on time only indirectly, through the time dependence of the irradiance. In fact, this rate must also depend on the number of molecules available to be excited, that is, on the ground state population. It is for this reason that the analytic model cannot account for saturation effects that arise from depopulation of the ground state. In addition, the absence from (1) of a term describing the nonradiative decay of molecules from the first excited state back to the ground state carries the tacit assumption that the time scale for this decay is much longer than the laser pulse width. In much the same way, the absence of terms for the radiative upward transitions between the first and second excited states and for the nonradiative decays in the opposite direction implies a tacit assumption that the lifetime of the second excited state is negligibly short. This last assumption presents no problem, as a rule. On the other hand, neglecting nonradiative depopulation of the excited state is valid only in the case of (1) extremely short pulses or (2) an effective excited state of triplet spin multiplicity. Such a state would be populated by a combined process consisting of a radiative transition from the (singlet) ground state to a singlet excited state followed by a nonradiative transition to the effective triplet excited state on a time scale that is shorter than or comparable to the pulse width.

3 Incorporation of Ground State Saturation Effects: Two-Band Rate Equation Model

The seminal excited state absorption model described in the previous section falsely assumes that the rate of energy absorption by active molecules in the ground state is independent of the number density n_G of such molecules. A more realistic treatment replaces the constant α by $\sigma_G n_G(t)$, where σ_G is the ground state absorption cross-section. In this case, (1) and (2) become:

$$\frac{\partial n_1}{\partial t} = \frac{\sigma_G}{h\nu} n_G I \tag{6}$$

$$\frac{\partial I}{\partial z} = -(\sigma_G n_G + \sigma_1 n_1) I \tag{7}$$

Like (1), Equation (6) neglects

- nonradiative decays from the excited state back to the ground state (a valid approximation so long as the excited state lifetime is much longer than the pulse width); and
- radiative transitions from the first excited state to the second excited state and nonradiative decays from the second excited state back to the first (a valid approximation, provided the downward transition is so fast that molecules reaching the second excited level decay almost immediately to the first excited state).

Since the lifetime of second excited state is taken to be so short that this state is always essentially empty, the populations of the ground state and first excited state satisfy

$$n_G(t) + n_1(t) = n_0, \tag{8}$$

where n_0 is the total number density of absorbing molecules.

The ground state absorption cross-section σ_G is determined by extinction measurements at low irradiance levels and is related to the linear absorption coefficient by $\alpha = n_0 \sigma_G$. The quantity $F_s = h\nu/\sigma_G$ defines a natural scale for the fluence; we expect that saturation effects will become significant at fluence levels approaching F_s. For this reason, one frequently refers to F_s as the "saturation fluence."

Equations (6), (7), and (8) maybe integrated with respect to time by the same procedure employed before. The result, which appears in [13], is

$$\frac{\partial F}{\partial z} = -n_0 \left\{ \sigma_1 F + (\sigma_G - \sigma_1) F_s \left(1 - \exp[-F/F_s]\right) \right\}, \tag{9}$$

or, expressed in terms of the dimensionless quantities $f = F/F_S$, $x = \alpha z$, and $\varsigma = \sigma_1/\sigma_G$,

$$\frac{\partial f}{\partial x} = -\varsigma f - (1-\varsigma)\left(1 - e^{-f}\right).$$

This longitudinal integration, in contrast to the one in (4), cannot be performed analytically.

4 Improved Analytic Model

The weak saturation limit of (9) suggests a slight improvement in the seminal excited state absorption model described in Section 2. At low fluence levels ($F / F_S << 1$), one can expand the exponential function on the right-hand side of (9) and so obtain

$$\frac{\partial F}{\partial z} = -\alpha F - \frac{\alpha(\sigma_1 - \sigma_G)}{2h\nu} F^2, \tag{10}$$

where we neglect terms of order $(F / F_S)^3$ and higher. This result is identical to (4), except that the quantity $\sigma_1 - \sigma_G$ in (10) plays the role of σ_1 in (4). Thus, the result (5) for the normalized transmittance must hold in this case, with the parameter q replaced by

$$q' = \frac{\alpha(\sigma_1 - \sigma_G)}{2h\nu} F_0 L_{eff} = \frac{1}{2}\left(\frac{\sigma_1}{\sigma_G} - 1\right)\frac{F_0}{F_S}\alpha L_{eff}.$$

To the best of our knowledge, this result is new and does not appear in the literature. It offers reasonable utility for fitting *Z*-scan data obtained with picosecond (or faster) pulses, for which fluence levels are considerably lower than for nanosecond pulses and for which the two-band model is generally a good approximation. This is discussed in more detail in Section 10.

5 A Comparison of the Simplest Excited State Absorption Models

For reasons that we presently discuss, one expects the two-band rate equation model described in Section 3 to fit the open aperture *Z*-scans of typical organic absorbers reasonably well, particularly if the curves in question are obtained using a picosecond (or faster) laser. For purposes of comparison with the two analytic models, both of which are limited by even more serious assumptions, we take the predictions of the two-band model to be "exact," as indeed they become on the appropriate time scales.

In contrast, the analytic "constant α" model of Wei et al. [4], reviewed in Section 2, presents obvious difficulties. As we have already mentioned, the approximation involved in characterizing ground state absorption by the linear absorption coefficient α, a constant, completely precludes saturable absorption. Every *Z*-scan curve computed with this model will have the "valley" shape characteristic of RSA, regardless of the relative values of the ground and excited state absorption cross-sections. This is because the constant α model, in effect, assumes that *all* the active molecules are constantly absorbing from the ground state, no matter how many of these are simultaneously ascribed to the excited state. This failure to account for the depletion of the ground state population as the excited state population grows also leads the constant α model to overstate the overall absorption of an RSA material with a given value of the excited state cross-section σ_1.

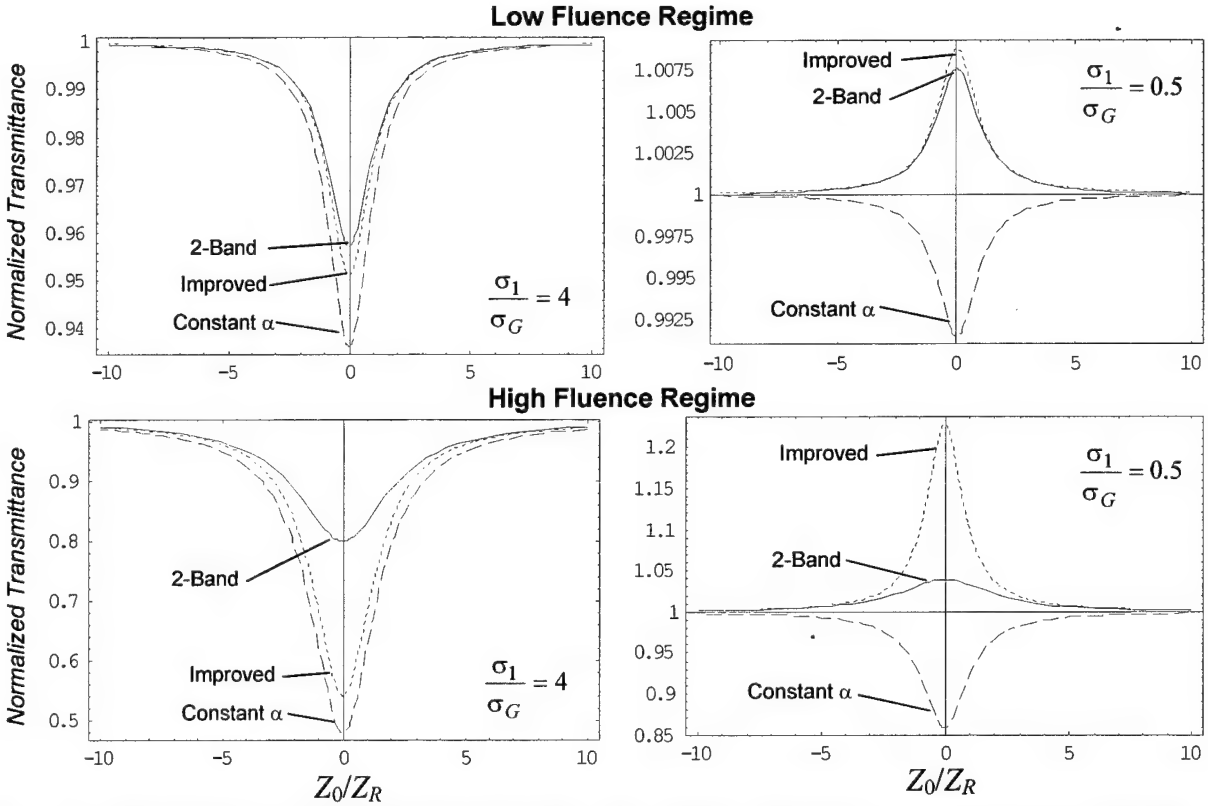

Figure 1. Theoretical *Z*-scan Curves Obtained From Various Excited State Absorption Models.

The improved model described in Section 4 is superior to the constant α model in both respects. It is capable of modeling saturable absorption, and it overstates the absorption of RSA materials to a lesser degree than the constant α model. Of course, the superiority of the improved model is expected to be greatest in the weak saturation limit.

The theoretical *Z*-scan curves displayed in Figure 1 graphically illustrate these points. All curves were calculated for a solution containing 10^{18} active molecules per cubic centimeter (equivalent to a 1.66-mM concentration). In every case, the ground state absorption cross-section σ_G was taken to be 10^{-17} cm^2, corresponding to a linear absorption coefficient α of 10 cm^{-1}. The left-hand pair of plots shows the theoretical curves predicted for a reverse saturable absorber having an excited state absorption cross-section σ_1 of 4×10^{-17} cm^2, while the two plots on the right show the curves for a saturable absorber with a σ_1 of 0.5×10^{-17} cm^2. As expected, the constant α model (long dashes) produces the same valley-shaped *Z*-scan characteristic of RSA, regardless of whether the material is saturably absorbing or reverse saturably absorbing.

The upper two plots in Figure 1 depict low-fluence *Z*-scans such as might be obtained from a 532-nm, principal-mode Gaussian beam delivering 100 nJ/pulse. Such a beam provides an on-axis fluence of about 27 mJ/cm^2. Since this value never exceeds 74% of the saturation fluence of 37.3 mJ/cm^2, we would expect the approximation ($F / F_S << 1$) that gave rise to the improved model to hold fairly well. In this case, the curves generated by the improved model (short dashes) do indeed show good agreement with the "exact" curves obtained from the two-band model (solid lines) for both saturably absorbing (top right plot) and reverse saturably absorbing materials (top left plot). On the other hand, the lower two plots illustrate the various models' predictions for *Z*-scans at fluence levels corresponding to an energy of 2 μJ/pulse, which is fairly typically for a *Z*-scan performed with a nanosecond laser. Assuming a spatial beam shape that is principal-mode Gaussian, such a pulse provides a fluence on axis of about 550 mJ/cm^2. This exceeds the saturation fluence by a factor of almost 15, so our expectations for the improved model should not be particularly high.

6 The Five-Band Model

Nonlinear absorption in a wide variety of organic materials, including the metallo-phthalocyanines and metallo-naphthalocyanines which have been the focus of so much recent attention, is well described by the five-band model depicted schematically in Figure 2. Each molecule is assumed to lie in the vibration-rotation manifold of one of five electronic states: the ground state, S_0; one of two excited singlet states, S_1 or S_2; or one of two excited triplet states, T_1 or T_2. Let σ_G, σ_S, and σ_T denote, respectively, the absorption cross sections for the transitions $S_0 \rightarrow S_1$, $S_1 \rightarrow S_2$, and $T_1 \rightarrow T_2$, and let k_S, k_{S2}, k_T, k_{T2}, and k_{isc} be the rate constants for the decays $S_1 \rightarrow S_0$, $S_2 \rightarrow S_1$, $T_1 \rightarrow S_0$, $T_2 \rightarrow T_1$, and $S_1 \rightarrow T_1$.

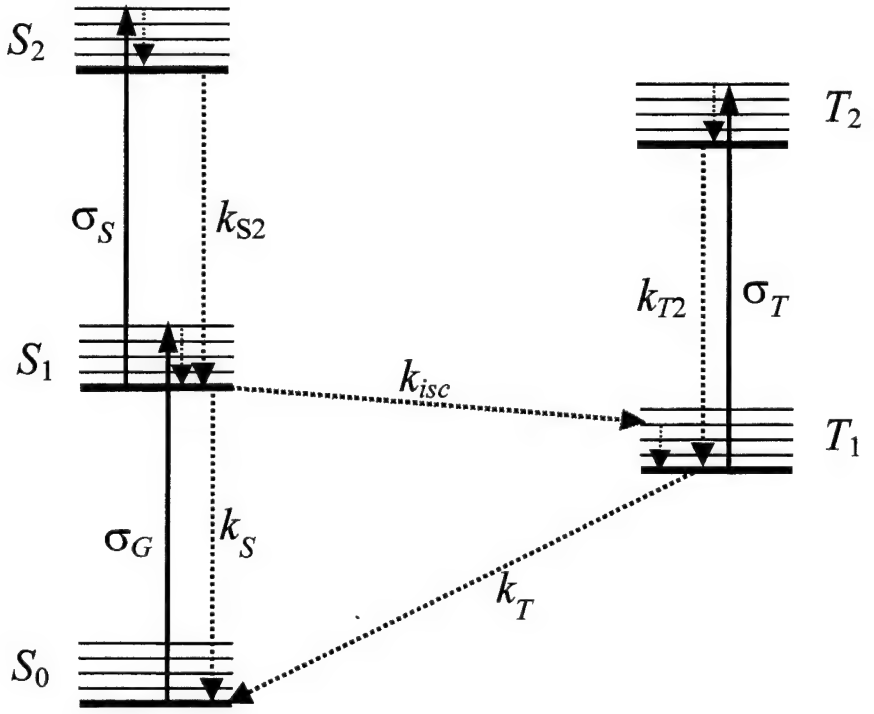

Figure 2. Five-band Model.

The following rate equations specify the time evolution of the number densities of molecules in the S_0, S_1, S_2, T_1, and T_2 bands; we refer to these number densities as "populations" and denote them by n_G, n_S, n_{S2}, n_T, and n_{T2}, respectively.

$$\frac{\partial n_G}{\partial t} = -\frac{\sigma_G}{h\nu} n_G I + k_S n_S + k_T n_T \tag{11}$$

$$\frac{\partial n_S}{\partial t} = \frac{\sigma_G}{h\nu} n_G I - (k_S + k_{isc}) n_S - \frac{\sigma_S}{h\nu} n_S I + k_{S2} n_{S2} \tag{12}$$

$$\frac{\partial n_T}{\partial t} = k_{isc} n_S - k_T n_T - \frac{\sigma_T}{h\nu} n_T I + k_{T2} n_{T2} \tag{13}$$

$$\frac{\partial n_{S2}}{\partial t} = \frac{\sigma_S}{h\nu} n_S I - k_{S2} n_{S2} \tag{14}$$

$$\frac{\partial n_{T2}}{\partial t} = \frac{\sigma_T}{h\nu} n_T I - k_{T2} n_{T2} \tag{15}$$

As before, ν is the frequency of the laser radiation, h is the Planck constant, and I the irradiance. Summing these equations, one verifies that they are consistent with the condition that n_0, the total number of molecules per unit volume,

$$n_0 = n_G + n_S + n_T + n_{S2} + n_{T2}, \tag{16}$$

be constant in time. Equation (16) may be used to eliminate one of the number densities (n_{T2}, say) from Equations (11) through (15). The rate equations for the five-band model thus consist of a system of four coupled ordinary differential equations in four unknowns.

We stress the fact that Equations (11) through (15) describe a "five-band model" as opposed to a "five-level model." This is because radiative transitions, such as the singlet-singlet transition from the ground state to the S_1 band, usually result in excitation high into the vibration-rotation manifold of the target electronic band, followed by a rapid decay to a state at the bottom of the band. This latter state is nonresonant with the incident radiation. As a result, stimulated emission terms are absent from (11) through (15).

Transitions between singlet and triplet states are forbidden by spin selection rules; the lifetime $\tau_T = k_T^{-1}$ of the lowest lying triplet state T_1 is thus extremely long, on the order of microseconds. In contrast, the effects of spin-orbit coupling induced by the metal substitute in metallo-phthalocyanines and metallo-naphthalocyanines combine with the closeness in energy of the S_1 and T_1 bands to shorten the decay time $\tau_{isc} = k_{isc}^{-1}$ for the intersystem crossing to several nanoseconds.

In certain organic compounds such as fullerenes [8, 9, 17] and cubanelike transition-metal clusters [11], there is evidence that the dominant mechanism by which the triplet manifold is populated is *not* intersystem crossing but rather, a process of ionization and subsequent germinate recombination. In this case, the band labeled S_2 in Figure 2 actually represents an ionized state of the molecule. The following modifications are required to adapt the rate Equations (11) through (15) to systems in which the triplet manifold is populated primarily by ionization followed by germinate recombination:

- One replaces the last term on the right-hand side of (12), $k_{S2} n_{S2}$, by $\pi_S k_{ion-e} {n_{S2}}^2$.
- One replaces the last term on the right-hand side of (14), $-k_{S2} n_{S2}$ by $-(\pi_S + \pi_T) k_{ion-e} {n_{S2}}^2$.
- An additional term $\pi_T k_{ion-e} {n_{S2}}^2$ is added to the right-hand side of (13).

Here, k_{ion-e} is the rate constant for cation-electron recombination and π_S and π_T are the probabilities of re-forming the molecule in the S_1 and T_1 state, respectively. (The probability of re-

forming molecules in the ground state by germinate recombination is so small that it may be safely ignored [17].)

Completing the five-band model is the following extinction law, which describes the decrease in intensity of the propagating beam as a result of linear and nonlinear absorption:

$$\frac{\partial I}{\partial z} = -(\sigma_G n_G + \sigma_S n_S + \sigma_T n_T) I . \tag{17}$$

7 The Truncated Five-Band Model

One can frequently simplify the five-band model by assuming that the populations of the S_2 and T_2 bands remain at a constant and negligible level [13]. Except at extremely high irradiances, this approximation should be generally valid. It represents an enormous simplification, allowing us to neglect the last two terms on the right-hand sides of (12), (13), and (16) and to ignore Equations (14) and (15) entirely. The resulting rate equations are

$$\frac{\partial n_G}{\partial t} = -\frac{\sigma_G}{h\nu} n_G I + k_S n_S + k_T n_T \tag{18}$$

$$\frac{\partial n_S}{\partial t} = \frac{\sigma_G}{h\nu} n_G I - (k_S + k_{isc}) n_S \tag{19}$$

$$\frac{\partial n_T}{\partial t} = k_{isc} n_S - k_T n_T \tag{20}$$

Using the following molecule conservation equation,

$$n_0 = n_G + n_S + n_T , \tag{21}$$

one may eliminate one of the number densities from Equations (18) through (20). The irradiance is described by (17), the same extinction law as the five-band model. We refer to the model defined by (17) through (21) as the *truncated five-band model*.

8 Validity of Second Excited Band Truncation

In order to examine the limitations imposed by the approximation described in the preceding section, we use the full set of rate equations, (11) through (15), to compute the evolution in time of the relative number densities of molecules in each of the five bands. Figure 3 shows the number densities on the input face of a sample of silicon naphthalocyanine (SiNc) illuminated by a laser pulse of Gaussian temporal profile and full width at half maximum (FWHM) pulse width 100 ps (upper pair of graphs) and 10 ns (lower graph). We performed these computations by taking $k_{S2} = k_{T2} = (1\text{ ps})^{-1}$, $k_T = (300\text{ ns})^{-1}$, and employing newly published values for the remaining rate constants and the absorption cross-sections [18]. At these peak intensities (2 GW/cm^2 for the 100-ps pulse and 1 GW/cm^2 for the 10-ns pulse, corresponding respectively to fluences of 0.2 J/cm^2 and 10 J/cm^2 on axis), the population of the T_2 band is *not* negligible relative to that of the T_1 band, nor is the S_2 population negligible relative to the S_1 population.

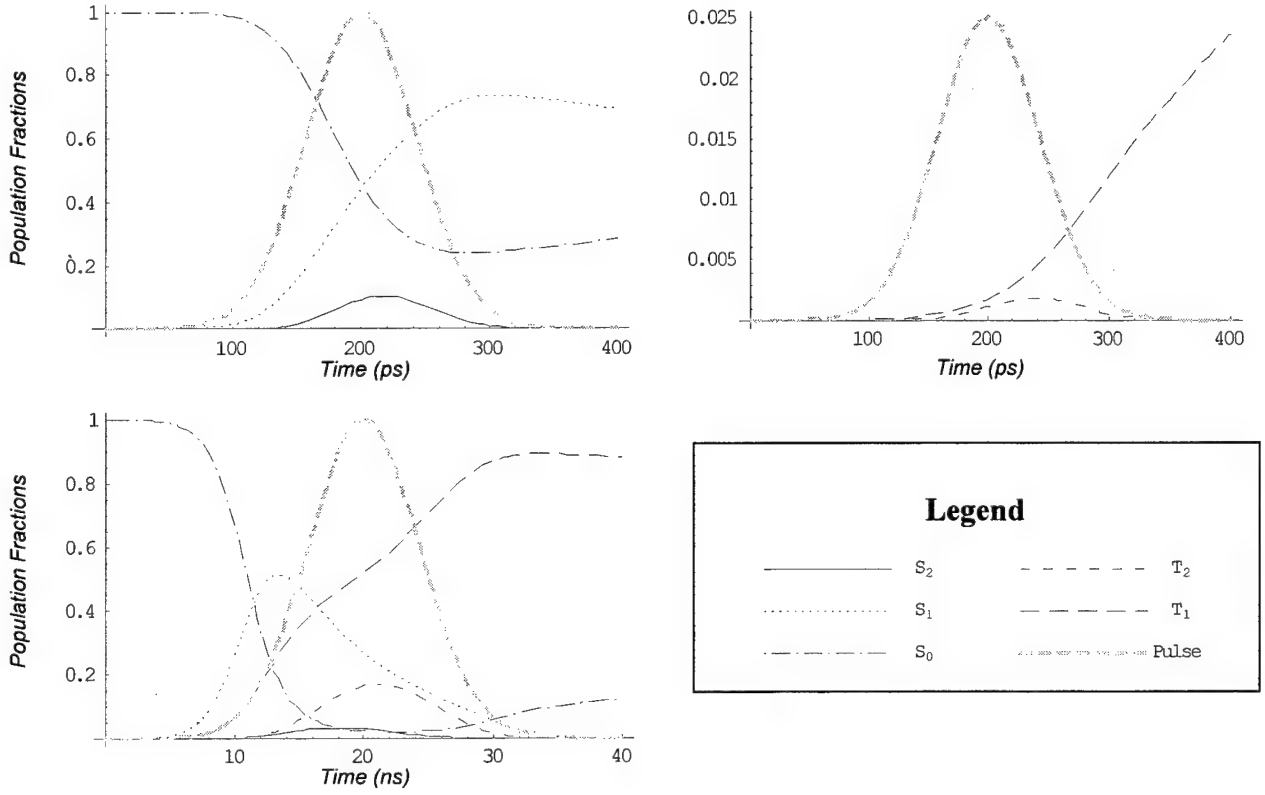

Figure 3. Band Population Fractions at the Input Face of a Sample of SiNc.

9 Full and Truncated Five-Band Models Compared: Excited State Saturation

Because it takes the lifetimes of the second excited states to be vanishingly small and thus precludes excited state saturation, the truncated model overstates excited state absorption. In principle, the values of excited state absorption cross-sections extracted from open aperture *Z*-scan data via the truncated model will lie below their true values. In practice, this discrepancy is completely negligible, since *Z*-scan experiments are typically performed at such low intensities that the normalized transmittance computed with the truncated model differs only slightly from that calculated with the exact model, the difference being most pronounced for the portion of the curve near the focal plane. This situation is well illustrated in Figure 4. Shown are the theoretical Z-scan curves for a 1.89-mM SiNc sample, 0.1 mm thick. The upper curve is calculated with the full five-band model and the lower curve, with the truncated model. Both computations assume a laser source at 532 nm delivering 7.25 μJ per 7.12-ns FWHM Gaussian pulse. The beam is assumed to be a principal-mode ($TEM_{0,0}$) Gaussian beam, focused to a spot of radius 10.8 μm.

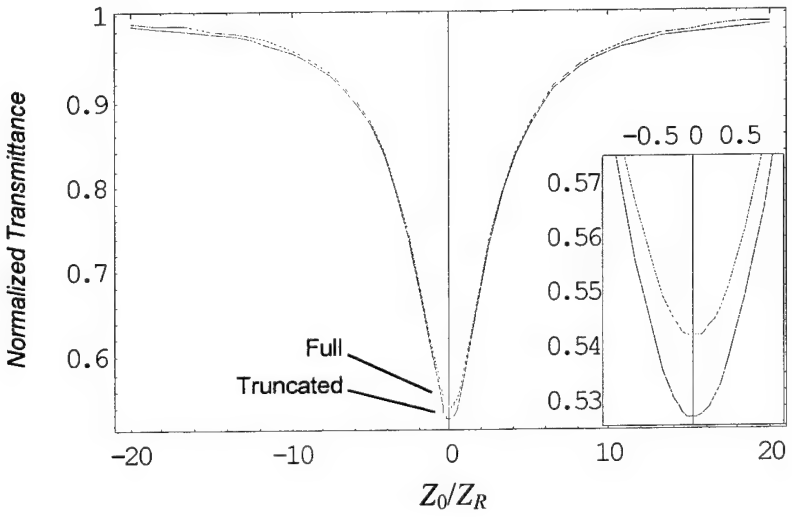

Figure 4. Z-scan Curves Obtained with Full and Truncated Five-band Models.

In modeling power limiting, however, the situation is very different, as Figure 5 illustrates. The power limiting curves shown in Figure 5 are for a 0.1-mm sample of SiNc. The upper solid curve was calculated with the full five-band model, while the lower solid curve employed the truncated five-band model. The dotted curve shown in the plot on the right extrapolates low-energy transmission. In this case, the "exact" full five-band model predicts a decline in excited state absorption resulting from excited state saturation. Of course, one might argue that at the fluence levels where the discrepancy between the two models becomes significant, modeling efforts are already problematic due to the onset of a host of processes that are not yet well quantified, such as plasma and bubble formation.

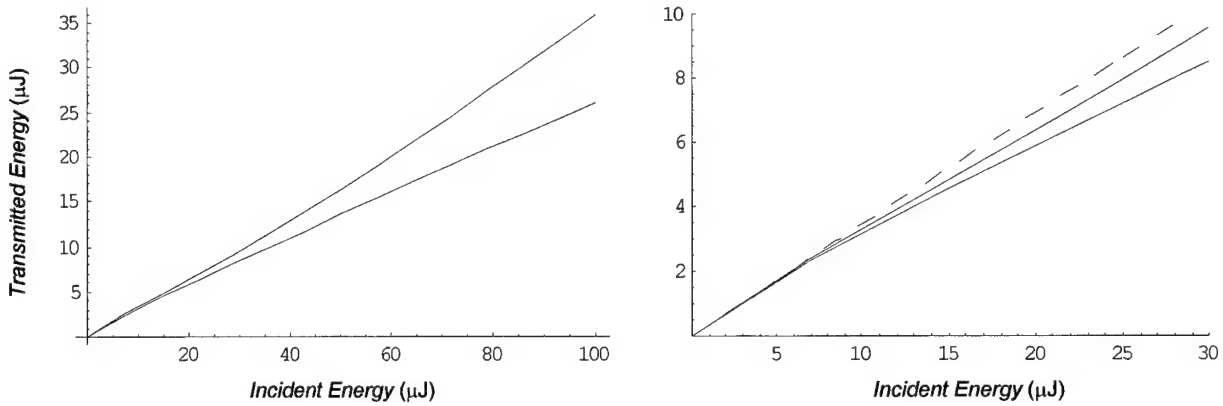

Figure 5. Power Limiting Curves for the Full and Truncated Five-band Models.

The computational savings that may be realized by employing the truncated version of the five-band model instead of the full version are less significant than one might think. Displayed in Table 1 are some representative results for the normalized transmittance, obtained during the calculation of *Z*-scan curves just discussed, along with the computation time required for each.

Table 1. Relative Computation Times for the Full and Truncated Five-band Models

	Full		***Truncated***	
$\frac{Z}{Z_R}$	$\frac{T}{T_L}$	**Time (s)**	$\frac{T}{T_L}$	**Time (s)**
0	0.54159	3177	0.52661	3238
1	0.59610	3559	0.58772	2935
5	0.87425	3092	0.87086	2296
10	0.95993	3072	0.95645	2227

10 Two- and Three-Band Effective Models

For the appropriate time scales, the five-band rate equation model can be simplified by the omission of an entire manifold of electronic states. For instance, in the case of picosecond pulses, the triplet states are always essentially empty and the system is well described by a three-band model with a single excited state with absorption cross section $\sigma_1 = \sigma_S$. Conversely, for long pulses (pulse widths $\tau_{pulse} >> \tau_{isc}$) and continuous wave beams, one may choose to ignore the effects of the $S_1 \rightarrow S_2$ transition, particularly when $\sigma_T >> \sigma_S$, as is frequently the case. In such instances, one often adopts a three-band model with $\sigma_1 = \phi\sigma_T$, where the triplet yield ϕ is the fraction of the excited singlet population which reaches the triplet state. And even when *both* the singlet-singlet and triplet-triplet excited state transitions are of comparable importance, it is always possible to define an effective excited state cross section in a quasi three-band model valid for a particular pulse width and fluence [13]. We wish to consider a generic situation in which there is a ground state and one, two, or more excited bands of unspecified spin multiplicity. Figure 6 depicts the situation with a pair of excited bands.

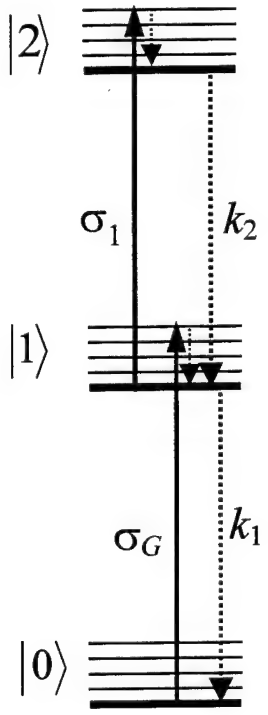

Figure 6. Three-band Effective Model.

The arguments from our discussion of the truncated five-band model in Section 7 apply equally well here. If the lifetime of the second excited band is sufficiently short (the usual situation unless the first and second excited bands differ in spin multiplicity), it is generally necessary to track the population of this band only in situations involving extremely high fluence levels. In all other cases, we are well served by the following truncated system of rate equations:

$$\frac{\partial n_G}{\partial t} = -\frac{\sigma_G}{h\nu} n_G I + k_1 n_1$$

$$\frac{\partial n_{es}}{\partial t} = \frac{\sigma_G}{h\nu} n_G I - k_1 n_1,$$

where k_1 is rate constant for decay from the excited state to the ground state. These two equations are equivalent, as can be easily seen from the condition (21) for conservation of absorber molecules, which in this case reads simply $n_0 = n_G + n_1$. The level populations in the resulting two-band effective model are thus described by a single differential equation, which is conveniently expressed in terms of the fraction X of molecules in the excited state ($X = n_1 / n_0$):

$$\frac{\partial X}{\partial t} = \frac{I}{F_s}(1 - X) - k_1 X . \tag{22}$$

Here, F_s is the saturation fluence, defined in Section 3 above, as $F_s = h\nu/\sigma_G$. The differential equation for the irradiance is

$$\frac{\partial I}{\partial z} = -n_0 \{\sigma_G (1 - X) + \sigma_1 X\} I . \tag{23}$$

The system of coupled equations (22) and (23) constituting the two-band model may be solved analytically in two special cases, which we now review in turn.

10.1 Negligible Excited State Decay

If the excited state lifetime τ_1 is much greater than the pulse width (as is the case for nanosecond pulses when the excited state is a triplet state), then τ_1 may be taken to be effectively infinite and $k_1 = \tau_1^{-1} = 0$. In this case, the two-band model reduces to the model developed in Section 3. Equation (22) may be integrated with respect to time to give

$$X(t) = 1 - \exp[-F(t) / F_s]$$

where

$$F(t) = \int_{-\infty}^{t} I(t')\, dt'$$

is the fluence at time t. Substituting the above expression for $X(t)$ in (23) and integrating the result over all time yields (9).

10.2 No Saturation

The other special case in which (22) and (23) may be solved analytically, while arising far less frequently in practice than the case of negligible excited state decay, is nonetheless applicable to a number of materials, notably indoaniline. It occurs when the ground and excited state

absorption coefficients are identical: $\sigma_G = \sigma_1 \equiv \sigma$. In this case, the overall absorption coefficient is strictly constant,

$$\alpha = \sigma_G n_G + \sigma_1 n_1 = \sigma(n_G + n_1) = \sigma n_0, \tag{24}$$

so the irradiance is independent of time and described by the familiar Beer's Law relation:

$$I(z) = I(z_0) e^{-\alpha(z-z_0)}.$$

Thus, (22) may be integrated to give

$$X(t) = \frac{1 - \exp\left[-\left(k_1 + \dfrac{I(z)}{F_s}\right)t\right]}{1 + \dfrac{k_1 F_s}{I(z)}} = \frac{1 - \exp\left[-\left(1 + \dfrac{I(z)}{I_s}\right)\dfrac{t}{\tau_1}\right]}{1 + \dfrac{I_s}{I(z)}},$$

where $\tau_1 = k_1^{-1}$ is the excited state lifetime and

$$I_s = k_1 F_s = \frac{h\nu}{\sigma\tau_1}.$$

The constant I_s is usually referred to as the "saturation intensity." (This designation is something of a misnomer in the present case, since the overall absorption exhibits no saturation!)

11 Conclusions

This report summarizes the most commonly seen models for excited state absorption. In these models, nonlinearity arises from the redistribution of absorber molecules among various available energy bands, the absorption cross-sections of which differ in magnitude. The existing analytic model for excited state absorption involves approximations that entirely preclude saturable absorption and lead one to underestimate the absorption cross-sections of reverse saturable absorbers based on their *Z*-scans. We present here an improved analytic model that is able to reproduce the behavior of saturable absorbers and that mitigates the degree to which model fits of *Z*-scan curves underestimate the excited state absorption cross-sections of reverse saturable absorbers.

The most complete description of the conjugated organic compounds currently under study as potential optical limiters is provided by a model involving five molecular energy bands and which we straightforwardly designate the *full five-band model*. One frequently assumes that the populations of the highest energy band of each spin multiplicity (*i.e.*, the S_2 and T_2 bands) remain at a constant and negligible level. This approximation gives rise to a model that we refer to as the *truncated five-band model*. Most of the theoretical calculations reported in the recent literature employ this latter model, which most authors refer to simply as the "five-band model." We demonstrate in this report that, at least at the center of the beam, the populations of the ignored bands are in fact non-negligible even at moderate fluence levels. These populations should definitely be included (through the use of the full five-band model) in the modeling optical limiter performance, though they may be safely ignored (by the use of the truncated model) in the interpretation of *Z*-scan data.

In modeling the propagation of nanosecond pulses, one is generally restricted to the use of either the full or truncated five-band model, assuming that the material to be modeled has an energy level structure consistent with the five-band scheme. For very short or very long pulses, additional simplifications are possible, and these give rise to two- and three-band effective models. An effective model may also prove useful in a preliminary attempt to elucidate the nonlinear optical behavior of materials having energy level structures that differ from the standard five-band arrangement.

References

[1] C. R. Guliano and L. D. Hess, "Nonlinear absorption of light: optical saturation of electronic transitions in organic molecules with high intensity laser radiation," *IEEE J. Quantum Electron.* ***QE-3***, 358-367 (1967).

[2] L. W. Tutt and S. W. McCahon, "Reverse saturable absorption in metal cluster compounds," *Opt. Lett.* ***15***, 700 (1990).

[3] G. R. Allan, D. R. Labergerie, S. J. Rychnovsky, T. F. Boggess, A. L. Smirl, and L. Tutt, "Picosecond reverse saturable absorption in King's complex," *J. Phys. Chem.* ***96***, 6313 (1992).

[4] T.-H. Wei, D. J. Hagan, M. J. Sence, E. W. Van Stryland, J. W. Perry, and D. R. Coulter, "Direct measurements of nonlinear absorption and refraction in solutions of phthalocyanines," *Appl. Phys.* ***B51***, 46-51 (1992).

[5] J. W. Perry, K. Mansour, S. R. Marder, K. J. Perry, D. Alvarez, Jr., and I. Choong, "Enhanced reverse saturable absorption and optical limiting in heavy-atom substituted phthalocyanines," *Opt. Lett.* ***19***, 625 (1994).

[6] L. W. Tutt and A. Kost, "Optical limiting performance of C_{60} and C_{70} solutions," *Nature* ***356***, 225-226 (1992).

[7] A. Kost, L. Tutt, M. B. Klein, T. K. Dougherty, and W. E. Elias, "Optical limiting with C_{60} in poly(methyl methacrylate)," *Opt. Lett.* ***18***, 334-336 (1993).

[8] F. Henari, J. Calaghan, H. Stiel, W. Blau, and D. J. Cardin, "Intensity-dependent absorption and resonant optical nonlinearity of C_{60} and C_{70} solution," *Chem. Phys. Lett.* ***199***, 144 (1992).

[9] D. G. McLean, R. L. Sutherland, M. C. Brant, D. M. Brandelik, P. A. Fleitz, and T. Pottenger, "Nonlinear absorption study in a C_{60}-toluene solution," *Opt. Lett.* ***18***, 858 (1993).

[10] G. L. Wood, M. J. Miller, and A. G. Mott, "Investigation of tetrabenzporphyrin by the Z-scan technique," *Opt. Lett.* ***20***, 973-975 (1995).

[11] W. Ji, H. J. Du, S. H. Tang, and S. Shi, "Nanosecond reverse saturable absorption in cuban-elike transition-metal clusters," *J. Opt. Soc. Am. B* ***12***, 876-881 (1995).

[12] P. A. Miles, "Bottleneck optical limiters: the optimal use of excited-state absorbers," *Appl. Opt.* ***33***, 6965-6979 (1994).

[13] T. Xia, D. J. Hagan, A. Dogariu, A. A. Said, and E. W. Van Stryland, "Optimization of optical limiting devices based on excited-state absorption," *Appl. Opt.* ***36***, 4110-4122 (1997).

[14] D. C. Hutchings, M. Sheik-Bahae, D. J. Hagan, and e. W. Van Stryland, "Kramers-Kronig relations in nonlinear optics," *Opt. Quantum Electron.* ***24***, 1-30 (1992).

[15] M. Sheik-Bahae, A. A. Said, and E. W. Van Stryland, "High-sensitivity, single-beam n_2 measurements," *Opt. Lett.* ***14***, 955-957 (1989).

[16] M. Sheik-Bahae, A. A. Said, T.-H. Wei, D. J. Hagan, and E. W. Van Stryland, "Sensitive measurement of optical nonlinearities using a single beam," *IEEE J. Quantum Electron.* ***26***, 760-769 (1990).

[17] G. A. Abakumov, V. B. Koloxksy, B. I. Polyakov, and A. P. Simonov, "Germinate and volume electron-cation recombination in a polyatomic buffer gas," *Chem. Phys. Lett.* ***182***, 321 (1992).

[18] S. N. R. Swatton, K. R. Welford, R. C. Hollins, and J. R. Sambles, "A time resolved double pump-probe experimental technique to characterize excited-state parametersof organic dyes," *Appl. Phys. Lett. 71(1)*, 10-12 (1997).

REPORT DOCUMENTATION PAGE

Form Approved
OMB No. 0704-0188

1. REPORT DATE *(DD-MM-YYYY)*	2. REPORT TYPE	3. DATES COVERED (From - To)
October 2002	Summary	Aug 00–Jul 01

4. TITLE AND SUBTITLE

Models for Saturable and Reverse Saturable Absorption in Materials for Optical Limiting

5a. CONTRACT NUMBER

5b. GRANT NUMBER

5c. PROGRAM ELEMENT NUMBER

6. AUTHOR(S)
Timothy Pritchett

5d. PROJECT NUMBER
1NE3AA

5e. TASK NUMBER

5f. WORK UNIT NUMBER

7. PERFORMING ORGANIZATION NAME(S) AND ADDRESS(ES)
U.S. Army Research Laboratory
Sensors and Electron Devices Directorate, ARL (ATTN: AMSRL-SE-EO)
White Sands Missile Range, NM 88002-5513

8. PERFORMING ORGANIZATION REPORT NUMBER
ARL-TR-2567

9. SPONSORING/MONITORING AGENCY NAME(S) AND ADDRESS(ES)
U.S. Army Research Laboratory
2800 Powder Mill Road
Adelphi, MD 20783-1145

10. SPONSOR/MONITOR'S ACRONYM(S)

11. SPONSOR/MONITOR'S REPORT NUMBER(S)
ARL-TR-2567

12. DISTRIBUTION/AVAILABILITY STATEMENT
Approved for public release; distribution unlimited.

13. SUPPLEMENTARY NOTES

The systems used to protect eyes and sensors from frequency-agile laser weapons must be capable, over a relatively broad range of frequencies, of absorbing, refracting, deflecting, or scattering laser radiation of high intensity, even while affording high transmission to light of low to moderate intensity. The design of such devices begins with an accurate characterization of the nonlinear optical response of the candidate active materials. In this work, the relevant material parameters can be extracted from experimentally obtained data only by indirect means: that is, the actual experimental results are compared to the results obtained from a theoretical model employing hypothetical values of the desired parameters, and the parameters of the model are varied until the model results match the experimental data. If this procedure is to work, the model must capture all the essential features of the interaction of the material to be characterized with the laser beam propagating through it. We review the assumptions and approximations underlying the commonly used models for nonlinear absorption, paying particular to the limits of applicability that these impose.

15. SUBJECT TERMS
Saturable, absorption, reverse saturable absorption, optical limiting, nonlinear optics.

16. SECURITY CLASSIFICATION OF:			17. LIMITATION OF ABSTRACT	18. NUMBER OF PAGES	19a. NAME OF RESPONSIBLE PERSON
a. REPORT	b. ABSTRACT	c. THIS PAGE			Timothy Pritchett
Unclassified	Unclassified	Unclassified	SAR		19b. TELEPHONE NUMBER *(Include area code)*